Nanobiology (1992) *1*, 457–468

Acousto-conformational Transitions in Cytoskeletal Microtubules: Implications for Intracellular Information Processing

ALEXEI SAMSONOVICH,[1,2] ALWYN SCOTT[1] AND STUART HAMEROFF[2]

[1]*Applied Mathematics Program, University of Arizona, Tucson, AZ 85724, USA*
[2]*Advanced Biotechnology Laboratory, Department of Anesthesiology, University of Arizona Medical Center, 1501 North Campbell Avenue, Tucson, AZ 85724, USA*

The hypothesis of long distance coherent, gigahertz-range excitations in the cytoskeleton and their possible role in energy/information conversion in living cells is supported by observations of gigahertz-range phonon excitations in proteins, sharp-resonant non-thermal effects of microwave electromagnetic irradiation on living cells and long-range regularities in cytoskeletal structures, such as the superlattice attachment patterns of microtubule associated proteins (MAPs) on microtubules. The latter is usually treated in terms of conformational changes of microtubule subunits. Using a Fröhlich-like model the present work numerically confirms that these conformational changes can be provoked by self-localized coherent phonon excitations whose original spectrum carries input information. The inherent phonon spectrum of the structure is then dependent on MAP locations and can function in a memory storage capacity. Such a system appears capable of adaptation and signal recognition involving spectrum–structure relations with feedback learning rules. Implications include intracellular information processing and molecular level electronic devices based on conformational phase transitions in protein arrays.

Keywords: *Coherent excitations, coherent phonons, cytoskeleton, Fröhlich excitations, information processing, microtubules, molecular computing, protein conformation, tubulin.*

1. INTRODUCTION

The existence of coherent, gigahertz-range oscillatory excitations in biomolecular structures and their possible role in living cells have been discussed in numerous theoretical proposals mainly based on the Fröhlich (1968) or Davydov (1981, 1985) approaches in connection with different components of living cells: membranes, individual proteins, actin filaments, etc (for review see Fröhlich, 1988; Fröhlich & Kremer, 1983; Golant, 1989). Although supportive experimental data are inconclusive, such organized excitations could explain a great deal regarding organization and information processing in living systems. In the present paper we are focussing on the possibility of coherent excitations in microtubules (MTs) (Hameroff, 1987; Rasmussen *et al.*, 1990).

MTs are the primary components of the cytoskeleton – intracellular networks of protein polymers which orchestrate cytoplasmic activities (Dustin, 1984). In contrast to other cytoskeletal elements, MTs have a non-trivial, periodic structure (Mandelkow *et al.*, 1986) and very long persistent length, about 1 μm (Dustin, 1984). These should result in a spectrum of global phonon modes. Corresponding patterns of standing waves in MTs can therefore be calculated in the

linear approximation from the symmetry of the structure (Figures 1 and 2, see Appendix for details).

There are at least two lines of indirect experimental evidence for the existence of coherent oscillatory phenomena in MTs within living cells:

(i) Neubauer *et al.* (1990) showed that 2.45 GHz irradiation non-thermally activates MT-mediated pinocytotic uptake in brain capillary endothelial cells ('blood−brain barrier function'). However, experimental data showing the effect directly at the molecular level are lacking (for general review of non-thermal microwave bioeffects, see Brown & Chattopadhyay, 1988;

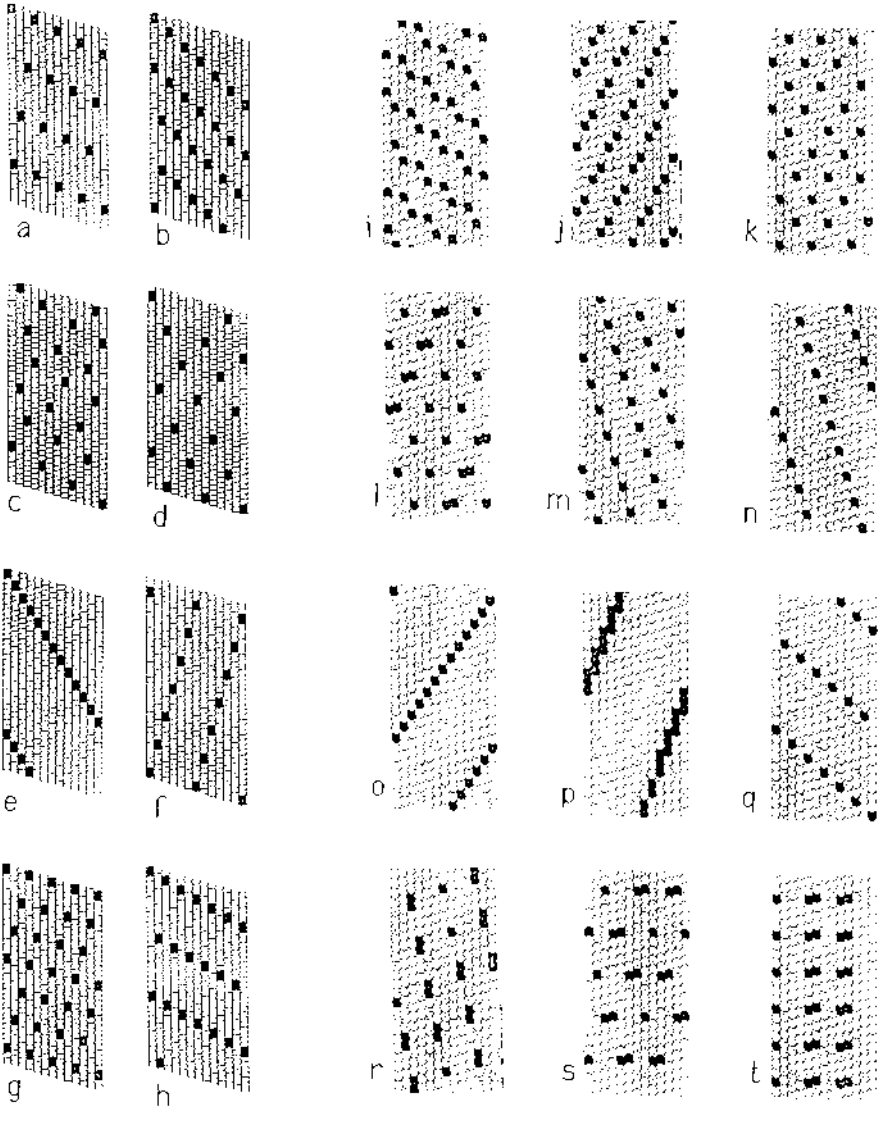

FIGURE 1. (*a*−*h*) Experimentally observed patterns of the MAP attachment sites on MTs (Burns, 1978; Kim *et al.*, 1986). Some of patterns (e and f) exactly coincide with patterns of the *ab initio* calculated phonon modes maxima (o and n). (*i*−*t*) Patterns of the MT phonon modes maxima, calculated according to (A9). Arrows at each site represent the complex amplitude of the related propagating mode (A7).

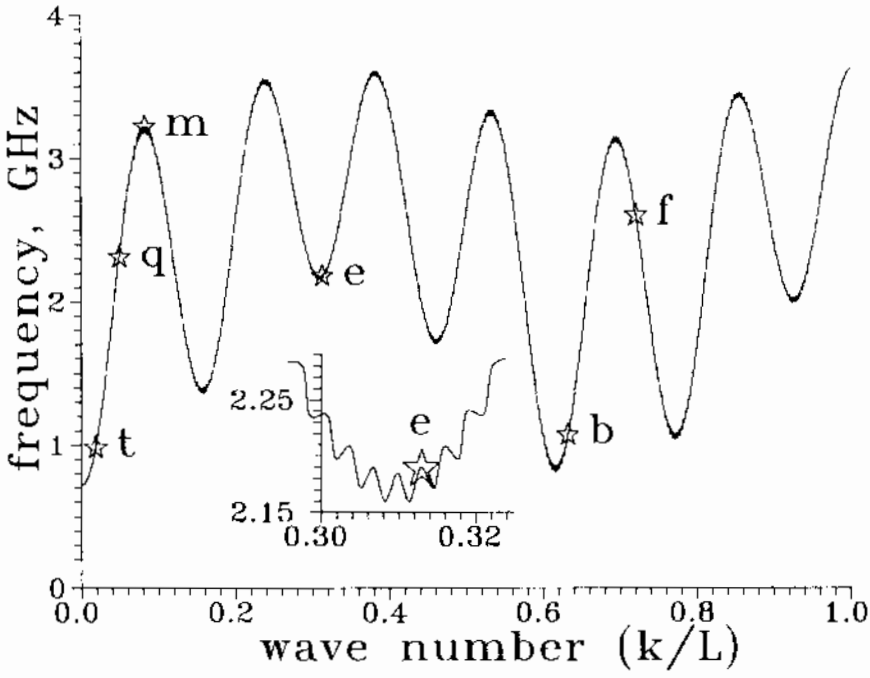

FIGURE 2. Phonon spectrum of the MT, calculated according to (A1), (A5) and (A9) for particular choice of the coupling constants (A10). Frequency in GHz. Labels show positions of some selected modes, represented at Figure 1.

Fröhlich, 1988; Golant, 1989). It is noteworthy that the action spectra of non-thermal microwave effects have sharp resonant lines with the corresponding quality factor of the order of 10^5 – 10^7 (Devyatkov *et al.*, 1973). This is difficult to understand in terms of biochemical reactions or non-pumped near-equilibrium molecular vibrational excitations, because quality factors or molecular oscillatory modes are usually less than 10^3 (Serikov & Khrisophorov, 1989; Genberg, 1991). However, living systems are usually far from thermal equilibrium. We know that MTs consume biochemical energy via GTP hydrolysis and phosphorylation. Hence, we can assume a certain pumping mechanism, which can provide self-excitation of molecular phonon/vibron modes. Thus we arrive at a Fröhlich-like model.

(ii) Other indirect evidence for oscillatory phenomena in MTs includes the existence of microtubule associated protein (MAP) attachment site superlattices on MTs (Figure 1), a feature which is well established but poorly understood (Kim *et al.*, 1986). The MAP attachment sites are MT tubulin subunits which differ from the others, apparently in their conformational state. This superlattice appears to be regular at large distances along the MTs, a fact difficult to understand in terms of local rules of superlattice formation involving static strains (Roth *et al.*, 1970) or MT self-assembling rules, due to finite probability of error.

Even more intriguing is the regularity of axopodial MT patterns (Cachon & Cachon, 1971; Bardele, 1977). One example of such structure is shown in Figure 3. The mechanism of morphogenesis of these patterns remains unknown. Different variants of linking between MTs in these structures imply different MAP superlattices existing at the same time in the same environment on different MTs, depending on their position in the structure. Earlier phenomenological explanations based on the gradion concept developed by Roth *et al.* (1970) involved graded conformational changes in MTs induced by static mechanical strains but appeared to be insufficient for understanding of the global symmetry (Bardele, 1977).

Hence, we can ask whether MAP attachment site pattern formation is controlled by a global

agent that is sensitive to geometry of the whole structure. One possible controlling candidate would be coherent phonon excitation since patterns of calculated phonon mode maxima prove to be similar to those of observed MAP attachment sites (Figure 1).

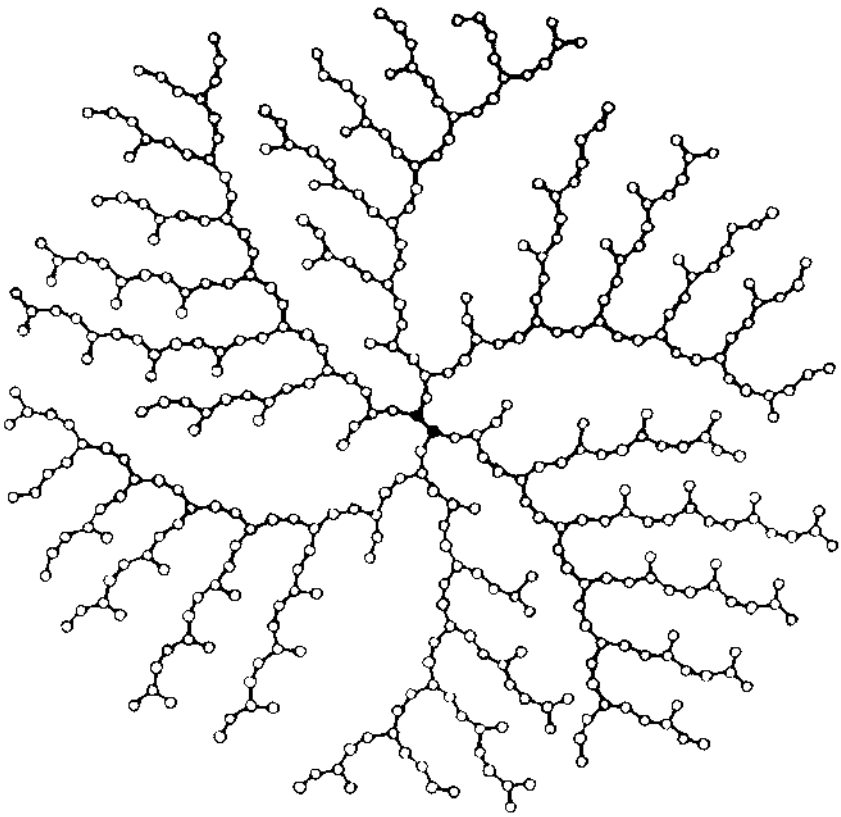

FIGURE 3. An example of MT cytoskeleton structure. Each circle is MT, links are MAPs (reprinted from Cachon *et al.*, 1971).

As for the pumping source for these modes, one candidate is bonded GTP hydrolysis which occurs at the GTP caps of growing MTs (Horio & Hotani, 1986). Another possibility concerns phosphorylation of MT subunits or of MAPs such as MAP2 (Theurkauf & Vallee, 1983).

The most interesting energy pumping mechanism may be conformational transitions of MT subunits occurring after MT assembly (Mandelkow *et al.*, 1983). It is natural to suppose that the energy of these chemical/conformational relaxations is mostly consumed by excitations of certain vibrational modes of the MTs rather than the environment: usually globular proteins relax in a quake-like motion (Frauenfelder *et al.*, 1988). In this case the rate of the conformational motion must depend on the vibrational excitation level, resulting in a simultaneous acousto-conformational transition (ACT) of the whole MT (or of its recently completed part). Such ACTs in MTs can be responsible for the MAP attachment site pattern formation and hence for cytoskeletal and cellular morphogenesis.

Each tubulin subunit is a globular protein with molecular weight about 55 kDa (Dustin, 1984), hence each subunit should possess a large set of vibrational freedoms. Some of them may result in global phonon modes of the MT, while others can remain local (Feddersen, 1991).

Conformational substates can also be described by certain freedoms (conformational coordinates) that in general should be strongly dissipative (Frauenfelder *et al.*, 1988). We can consider them as extensions of vibrational coordinates, thus the vibrational excitations can effect conformational transitions, and vice versa. Further, conformational changes usually shift frequencies of molecular oscillators (Frauenfelder *et al.*, 1990). Global (phonon) and local (vibron) excitations can be converted into each other due to non-linearity inherent in biomolecules.

In the present paper we describe this phenomenon in terms of the Fröhlich-like model (Fröhlich, 1968). This kind of model has been used for the vibrational analysis of polyatomic molecular structures (Eilbeck *et al.*, 1985) showing a variety of complicated non-linear dynamics, in particular phonon self-trapping. The questions now are: how does the vibrational pattern, which can be determined by the spectrum of the initial excitation, induce formation of a definite MAP attachment site superlattice on MTs, and what are the relationships between the initial spectrum and the final MAP attachment site superlattice? The answer is obtained numerically for a very simplified MT model.

2. THE PHYSICAL MODEL

Let us consider a model of the MT that is a linear chain of equivalent coupled oscillators, each possessing a set of freedoms.

Let the Hamiltonian model be

$$H = \sum_j \{w_0 a_j^+ a_j - \epsilon a_j^+ (a_{j-1} + a_{j+1}) - \Gamma a_j^+ a_j Q_j + \frac{P_j^2}{2M} + U(Q_j) + \lambda P_j (a_j^+ - a_j) + \sum_j \{w_j \alpha_j^+ \alpha_j + \chi a_j^+ a_j (\alpha_j^+ + \alpha_j)\}\} \tag{1}$$

where a_j^+ and a_j are creation and annihilation operators (becoming complex amplitudes in the classical theory) of 'global' vibrational modes; α_j^+ and $\alpha\sigma$ are those of the environment; Q_j and P_j are conformational conjugated coordinate and momentum, also describing 'local' vibrations, and the slope of the potential energy function $U(Q_j)$

$$U(Q) = \frac{K}{2}(Q^0 - Q)^2 + E_a \sin^2\left(\pi \frac{Q}{\Delta Q}\right), \quad E_a = M\Omega^2 \Delta Q^2 / 2\pi^2$$

is typical for globular proteins (Figure 4; see Frauenfelder *et al.*, 1988). Other coefficients (w, Γ, ϵ, M, λ, E_a, Ω, K, ΔQ) are phenomenological constants.

Supposing the local barriers heights E_a to be large compared with the temperature kT, we can assume that the system spends most of its time in the vicinity of local minima of U. Hence, we can separate conformational jumps occurring between these local minima from small vibrations occurring in the vicinity of these minima. Thus we can decompose Q into two sets of variables: slow discrete variables $\{q\}$, numbering the local minima of U, and fast variables $\{\tilde{Q} = Q \bmod \Delta Q\}$. In general we can consider these variables as vectors: $Q_j \equiv (Q_j^1, \ldots, Q_j^m)$, $q_j \equiv (q_j^1, \ldots, q_j^m)$, $\tilde{Q}_j = (\tilde{Q}_j^1, \ldots, \tilde{Q}_j^m)$, $P_j \equiv (P_j^1, \ldots, P_j^m)$, assuming appropriate tensor structure of the coefficients $1/2M$, Γ, λ and function U. Since we are interested in functionally important conformational motions (FIM) (Frauenfelder *et al.*, 1988), we can describe the 'macroscopic' conformational dynamics of the protein subunit by single quasicontinuous FIM coordinate q_j^i, assuming that the rest of q's are being taken into account in the entropy terms kTS of the free energy

$$F(q_j^i) = U(q_j^i) - kTS(q_j^i) = \frac{K}{2}(q_j^0 - q_j^i)^2. \tag{2}$$

Now we can represent (Q_j, P_j) pairs by complex vector amplitudes c_j^+ and c_j (becoming the creation and annihilation operators in the quantum theory) and rewrite the first line of (1) in

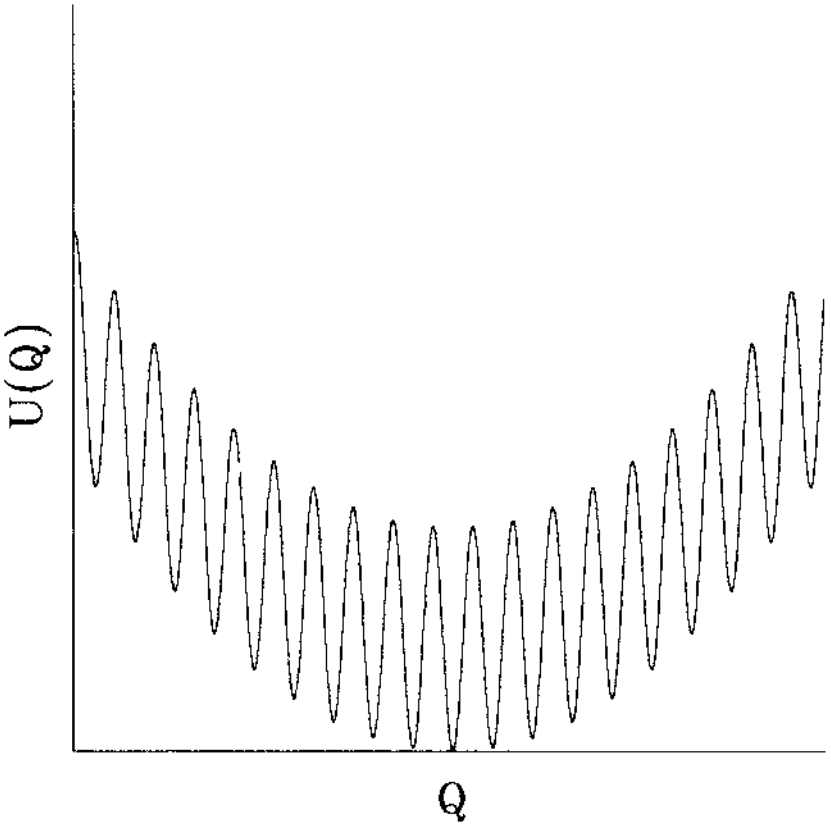

FIGURE 4. The free energy of a protein as a function of a conformational coordinate (see Frauenfelder *et al.*, 1990).

diagonal form, i.e. in terms of normal modes, calculated at fixed $\{q_i\}$:

$$c_i = (M\Omega\bar{Q}_i - iP_i) / \sqrt{2M\Omega} \tag{3}$$

$$\sum_i [w_{0i} a_i^+ a_i - \epsilon a_i^+ (a_{i+1} + a_{i-1}) \quad \Gamma a_i^+ a_i q_i^+] - \sum_k w_k b_k^+ b_k, \; w_k = w_k(w_0, \epsilon, \Gamma, \{q^+\}).$$

$$b_k = \sum_i u_{ki} a_i, \; a_i = \sum_k u_{ik}^{-1} b_k, \; \sum_k u_{ik}^{-1} u_{km} = \delta_{im}, \; u^+ = u = u(\{q^+\}) \tag{4}$$

$$H = H - \sum_k w_k b_k^+ b_k + \sum_i [\Omega c_i^+ c_i + F(q_i^+)]$$

$$+ \sum_{i,k} [\lambda \sqrt{2M\Omega}\, u_{ik}(c_i^+ b_k + c_i b_k^+) - \frac{\Gamma}{\sqrt{2M\Omega}} u_{ki}^+ u_{im} b_k^+ b_m (c_i^+ + c_i)]$$

$$+ \sum_j [w_j \alpha_j^+ \alpha_j + \tilde{\chi} \sum_{jk} b_k^+ b_k (\alpha_j^+ + \alpha_j)] \tag{5}$$

Finally we obtain from (5) the system of classical kinetic equations in terms of q_i^+ and the occupation numbers N_{bk}, N_{ci} in the mean field approximation, i.e. using the average values

$$N_{bk} = \langle b_k^+ b_k \rangle, \; N_{ci} = \sum_i \langle c_i^+ c_i^+ \rangle \tag{6}$$

Omitting irrelevant terms, we have

$$\dot{N}_{bk} = \varphi \sum_l f_{kl}(N_{cl} - N_{bk}) + \chi \sum_m g_{km} N_{bk} N_{bm} \mathrm{sign}(w_m - w_k)$$

$$\dot{N}_{cl} = -\varphi \sum_k f_{kl}(N_{cl} - N_{bk}) + \frac{K(q_l - q_l^0)}{\Omega} \dot{q}_l$$

$$\dot{q}_l = \mu_l K(q_l^0 - q_l^*) + \eta_l, \quad \langle \eta_l^2 \rangle = 2\mu\Omega N_{cl}, \quad \mu = A\exp(-E_a/\Omega N_{cl}) \tag{7}$$

where

$$f_{kl} = u_k^l u_{kl}, \quad g_{km} = \sum_l f_{kl} f_{lm} \tag{8}$$

The first two equations in (7) describe evolution of the phonon/vibron subsystem at given, slowly changing $\{q_l\}$. The last line in (7) is the Langevin equation, describing the diffusion in conformational space, influenced by the total vibrational excitation level N_{cl}. Here η is the Gaussian random force, and we make use of the Einstein relation between the mobility, μ and the diffusion coefficient $\langle \eta^2 \rangle / 2$, assuming 'thermalization' of local vibrations with effective temperature $kT_{ef} = \Omega N_{cl}$. The expression for μ is the Arrhenius relation taken from Frauenfelder *et al.* (1990), which has been established for certain FIM in myoglobin (in other cases the temperature dependence of μ is stronger). As for the phenomenological parameters (Ω, φ, χ, K, A, E_a), unfortunately, we have no possibility to estimate them from first principles. We only know that usually they can vary by many orders (Frauenfelder *et al.*, 1990).

Thus the task for numerical modeling can be formulated by equation (7) with initial conditions

$$N_{cl}(0) = N_{cl}^0, \quad N_{bk}(0) = N_{bk}^0, \quad q_l(0) = q_l^0 \tag{9}$$

3. NUMERICAL MODELING RESULTS

We have investigated the model (5)–(7) taking the following values of parameters (in dimensionless units; relation to physical scales is given in the Appendix):

$$w_0 = 5, \ \epsilon = 0.3, \ \varphi = 100, \ \chi = 200, \ KAq^0 = 50, \ E_a = 1, \ N_{cl}^0 = 0.01, \ N_{bk}^0 = 0.1 + 3\delta_{kk'} \tag{10}$$

where $\{k'\}$ represents the initial spectrum induced by external source.

The result is represented in Figure 5. It shows the known phenomena of Fröhlich Bose condensation into the ground state. We see that the total vibrational energy finally is localized at definite sites, predetermined by the initial spectrum. Thus the result is self-localization of phonons and fixation of the initially induced oscillatory pattern by ACT.

As for the true MT structure, we can suppose that the qualitative result will be the same. In this case the vibrational patterns can induce the known MAP attachment sites patterns on the MTs (see Figure 1).

4. DISCUSSION

Thus we have a mechanism which can provide a definite MAP attachment site pattern for each spectrum of initial excitation. Now we can discuss pattern self-reproduction in accordance with our model. Suppose we have two neighbouring coupled MTs (or two parts of the same MT), one of which has a fixed pattern of MAPs, while another is in a symmetric metastable state. The second subsystem can then undergo ACT: global coherent oscillations are initiated spontaneously by thermal fluctuations and amplified by energy release due to conformational motions stimulated by these oscillations. At the beginning of this process, only that mode can be excited which has the same pattern of maxima as the existing MAP superlattice of the rest of the system. Finally, this pattern of mode maxima can be converted into the MAP attachment sites pattern and then fixed by attachment of MAPs.

Another possibility consists of a global ACT, similar to a non-linear wave, propagating within

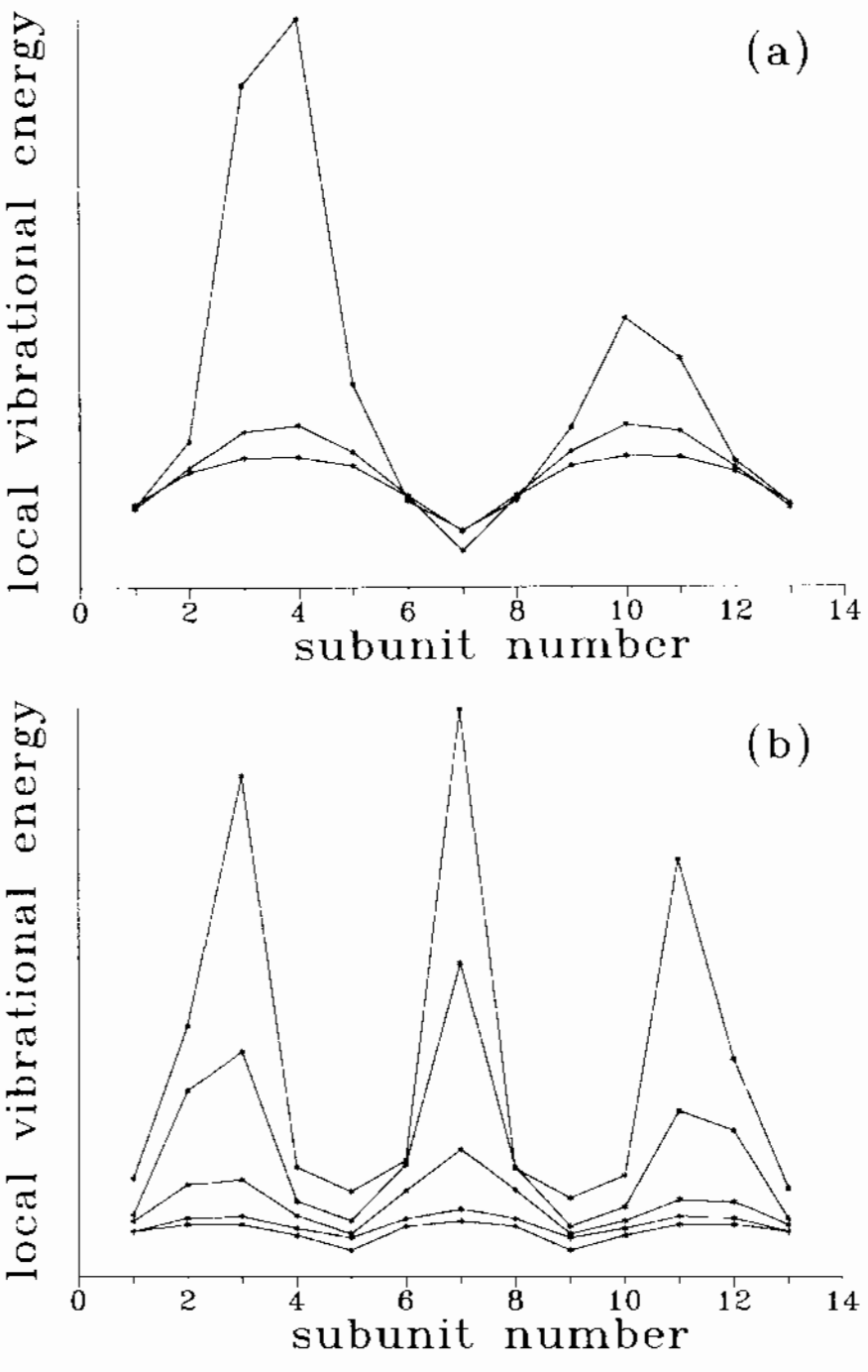

FIGURE 5. Time evolution of the vibrational energy distribution in the linear chain of coupled oscillators interacting with conformational freedoms for two different input signal spectra. Initially excited normal modes are: 2, 4, 6, 8, 10, 12 (a) and 3, 6, 9, 12 (b). One can see self-localization of energy at different patterns, predetermined by the spectrum of weak initial excitation.

cell along the cytoskeleton (and possibly from one cell to another). The initial metastability of the structure in this case can be provided by some changing in the environment (ionic, electric, pH, etc). The system of kinetic equations describing each step of this process is similar to those of non-linear neural network models with feedback (Carpenter & Grossberg, 1991): phonon excitations and conformational motions can be considered as a short-term memory, while attachment/disattachment of MAPs can provide a long-term memory. This analogy will be investigated elsewhere.

There are two interesting implications of this approach. The first concerns the cytoskeletal morphogenesis problem, such as the regular fractal MT patterns (Figure 3) and some inherent features of partially-ordered cytoskeletal architectures that are specific for certain kinds of cells (erythrocytes, fibroblasts, neurons, etc.) which can be transmitted from cell to cell (Alberts *et al.*, 1983). Within neurons, such architectures relate to synaptic regulation and plasticity, and may be important for learning, memory and cognitive function.

The second possible implication of these results concerns the adaptation ability of the cytoskeleton considered as an oscillatory network. It seems likely that nature uses this possibility for neuro-like information processing. At least, it may be possible to implement this principle in artificial molecular electronic devices based on protein arrays. A similar approach can be used as a technological tool in nanolithography: definite structures can be obtained by applying specific hypersound spectra.

Finally we arrive at the following conclusions:

(i) Periodical structure of MTs should result in a definite spectrum of global phonon mode maxima. Patterns of calculated phonon modes prove to be similar to those of observed MAP attachment sites (Figure 1, Appendix).

(ii) MAP attachment sites form a superlattice which keeps its pattern and orientation through long distances along MTs. This indicates the existence of some global agent involved in the process of superlattice formation.

(iii) The process of MAP attachment site superlattice formation is generally assumed to depend on the conformational transition of MTs. Conformational transitions in globular proteins are known to depend on (and are stimulated by) vibrational excitations of the protein. The same thing should take place in extended protein structures like MTs. Hence, vibrational (phonon) excitations of MTs can be the global agent orchestrating MT conformational transition, resulting in MAP attachment site formation. Thus we arrive at the concept of ACT.

(iv) A Fröhlich-like model can be used for description of ACT in MTs.

(v) Numerical study of ACT in MTs shows that the spectrum and the related spatial pattern of weak initial phonon excitation can determine the way of ACT, which involves phonon self-trapping at definite sites becoming MAP attachment sites. This result may explain sharp resonances in the action spectra of non-thermal microwave effects.

(vi) After attachment of MAPs at the MAP attachment sites, the structure acquires new phonon spectrum (related with the attached MAP pattern), which can determine the spectrum of initial phonon excitation preceding ACT in the neighboring cytoskeletal fragment. Thus features of the cytoskeletal architecture can be self-reproduced. This phenomenon can be used by living systems for intracellular information transmission during morphogenesis and/or during learning process in neurons.

(vii) ACT seem to be inherent phenomena for a wide variety of extended biomolecular structures, including artificial protein arrays. Thus they may be used for neuro-like information processing in molecular level electronic devices as well as for new methods in nanotechnology.

ACKNOWLEDGEMENTS

This study was supported by NSF grant number DMS-9114503. We are grateful to Alexander Bershadsky, Alexander Serikov, Steen Rasmussen and Rafael Lahoz-Beltra for valuable discussions.

REFERENCES

ALBERTS, B., BRAY, D., LEWIS, J., RAFF, M., ROBERTS, K. & WATSON, J.D. (1983) *Molecular Biology of the Cell*, 2nd edn. Garland, New York.

BARDELE, C.F. (1977) Comparative study of axopodial microtubule patterns and possible mechanisms of pattern control in the Centrohelidian Heliozoa Acanthocystis, Raphidiophrys and Heterophrys. *Journal of Cell Science* **23**, 205–232.

BROWN, H.D. & CHATTOPADHYAY, S.K. (1988) Electromagnetic field exposure and cancer. *Cancer Biochemistry and Biophysics* **9**, 295–342.

BURNS, R.B. (1978) Spatial organization of the microtubule associated proteins of reassembled brain microtubules. *Journal of Ultrastructure Research* **65**, 73–82.

CACHON, PAR J. & CACHON, M. (1971) The axopodial systems of *Radiolaria nassolaria*. *Archiv für Protistenkunde* **113**, 80–97.

CACHON, PAR J., CACHON, M., FEBVRE-CHEVALIER, C. & FEBVRE, J. (1973) Theoretical models for microtubular systems of Actinopod axopods. *Archiv für Protistenkunde* **115**, 137–153.

CARPENTER, G. A. & GROSSBERG, S., eds (1991) *Pattern Recognition by Self-organizing Neural Networks*. MIT Press, Cambridge.

DAVYDOV, A. S. (1981) *Biology and Quantum Mechanics*. Pergamon Press, Oxford.

DAVYDOV, A. S. (1985) *Solitons in Molecular Systems*. Kluwer, Dordrecht.

DEVYATKOV, N.D. (1973) Influence of millimeter-band electromagnetic radiation on biological objects. *Soviet Physic Uspekhi* **16**, 568–569.

DUSTIN, P. (1984) *Microtubules*, 2nd revised edn. Springer-Verlag, Berlin.

EILBECK, J.C., LOMDAHL, P.S. & SCOTT, A.C. (1985) The discrete self-trapping equation. *Physica D* **16**, 318–338.

FEDDERSEN, H. (1991) Localization of vibrational energy in globular protein. *Physics Letters A* **154**, 391–395.

FRAUENFELDER, H., PARAK, F. & YOUNG, R.D. (1988) Conformational substates in proteins. *Annual Review of Biophysics and Biophysical Chemistry* **17**, 451–479.

FRAUENFELDER, H., ALBERDING, N.A., ANSARI, A., BRAUNSTEIN, D., COWEN, B.R., HONG, M.K., IBEN, E.T., JOHNSON, J.B., LUCK, S., MARDEN, M.C., MOURANT, J.R., ORMOS, P., REINISCH, L., SCHOOL, R., SCHULTE, A., SHYAMSUNDER, E., SORENSEN, L.B., STEINBACH, P.J., XIE, A., YOUNG, R.D. & YUE, K.T. (1990) Proteins and pressure. *Journal of Physical Chemistry* **94**, 1024–1037.

FRÖHLICH, H. (1968) Long range coherence and energy storage in biological systems. *International Journal of Quantum Chemistry* **2**, 641–649.

FRÖHLICH, H. Ed. (1988) *Biological Coherence and Response to External Stimuli*. Springer-Verlag, Berlin.

FRÖHLICH, H. & KREMER, F. (1983) *Coherent Excitations in Biological Systems*. Springer-Verlag, Berlin.

GENBERG, L., RICHARD, L., MCLENDON, G. & MILLER, R.J.D. (1991) Direct observation of global protein motion in hemoglobin and myoglobin on picosecond time scales. *Science* **251**, 1051–1054.

GOLANT, M.B. (1989) Resonance action of coherent electromagnetic millimetre waves on living organisms. *Biofizika* **34**, 338–348.

GOLANT, M.B. (1989) Resonance effect of coherent electromagnetic radiations of millimetre range of waves on the living organisms. *Biofizika* **34**, 1004–1014.

GRUNDLER, W., KEILMANN, F. & FRÖHLICH, H. (1971) Resonant growth rate response of yeast cells irradiated by weak microwaves. *Physics Letters A* **62**, 643–646.

HAMEROFF, S.R. (1987) *Ultimate Computing*. Elsevier North Holland, Amsterdam.

HORIO, T. & HOTANI, H. (1986) Visualization of the dynamic instability of individual microtubules by dark-field microscopy. *Nature* **321**, 605–607.

KIM, H., JENSEN, C.G. & RUBIUND, L.I. (1986) The binding of MAP-2 and tau on brain microtubules *in vitro*: implications for microtubule structure. *Annals of the New York Academy of Sciences* **466**, 218–239.

MANDELKOW, E-M., SCHULTHEISS, R., RAPP, R., MULLER, M. & MANDELKOW, E. (1986) On the surface lattice of microtubules: helix starts, protofilament number, seam, and handedness. *Journal of Cell Biology* **102**, 1067–1073.

MANDELKOW, E., MANDELKOW, E.-M. & BORDAS, J. (1983) Synchrotron radiation as a tool for studying microtubule self-assembly. *Trends in Biochemical Sciences* **8**, 374–377.

NEUBAUER, C., PHELAN, A.M., KUES, H. & LANGE, D.G. (1990) Microwave irradiation of rats at 2.45 GHz activates pinocytotic-like uptake of tracer by capillary endothelial cells of cerebral cortex. *Bioelectromagnetics* **11**, 261–268.

RASMUSSEN, S., KARAMPURWALA, H., VAIDYANATH, R., JENSEN, K.S. & HAMEROFF, S. (1990) Computational connectionism within neurons: a model of cytoskeletal automata subserving neural networks. *Physica D* **42**, 428–449.

ROTH, L.E. PIHLAJA, D.J. & SHIGENAKA, Y. (1970) Microtubules in the heliozoan axopodium. I. The gradion hypothesis of allosterism in structural proteins. *Journal of Ultrastructure Research* **30**, 7–37.

SERIKOV, A.A. & KHRISTOPHOROV, L.N. (1989) *ITP Preprint-89*. Institute for Theoretical Physics Ukrainian Academy of Sciences. Kiev.

THEURKAUF, W.E. & VALLEE, R.B. (1983) Extensive cAMP-dependent and cAMP-independent phosphorylation of microtubule associated protein 2. *Journal of Biological Chemistry* **258**, 7883–7886.

APPENDIX: MT NORMAL MODES CALCULATION

Here we study the MT phonon modes in the linear approximation, which should be used when the vibrations are initialized by some (external) source, hence, their amplitudes are small. For the sake of simplicity, let us consider each MT dimer subunit as a one-freedom harmonical oscillator, linearly coupled with its six nearest neighbors. Recollecting well-known data about the MT structure (Dustin, 1984; Mandelkow, 1986), it is natural to assume original equivalence of all subunits (here we disregard the MT dislocation line). Thus, for MTs with 13 protofilaments, three-start helix and A-lattice (Mandelkow, 1986) we have the following Hamiltonian with four independent parameters (w_0, ϵ_1, ϵ_2, ϵ_3):

$$H = \sum_l \{w_0 a_l^* a_l \quad \epsilon_1 a_l^* (a_{l-13} + a_{l+13}) - \epsilon_2 a_l^* (a_{l-10} + a_{l+10}) \tag{A1}$$

$$- \epsilon_3 a_l^* (a_{l-3} - a_{l+3})\} = \sum_{l,l'} a_l^* H_{ll'} a_{l'}$$

where $H_{ll'}$ is the Hamiltonian matrix, and a_l^* and a_l are complex vibrational amplitudes:

$$a_l = \frac{1}{\sqrt{2Mw_0}} (Mw_0 q_l - ip_l) \tag{A2}$$

q_l and p_l are the l-th oscillator conjugated coordinate and momentum, M the subunit effective mass. We make use of the site number l, supposing all sites to be numbered in the longitudinal direction as

$$l = 13i + 3j, \quad x - l \cdot a/13 \approx (0.615 \text{ nm}) \cdot l \tag{A3}$$

where i and j are discrete longitudinal and transversal coordinates of the site, x the physical longitudinal coordinate of the site and $a = 8$ nm is the MT lattice spacing.

According to classical mechanics, the stationary states, or the phonon normal modes of the system, $\{a_l^k(t)\}$, should be the solutions of the eigenvector problem:

$$\sum_{l'} H_{ll'} a_{l'}^k = w_k a_l^k \tag{A4}$$

with the Hamiltonian matrix given by (A1). We can represent them in terms of the unitary matrix u, which diagonalizes the Hamiltonian matrix:

$$a_l^k(t) = u_{lk} b_k \exp(iw_k t) \tag{A5}$$

$$u^+ H u = \text{diag}(w_1, \ldots, w_L), \; u^+ u = 1 \tag{A5a}$$

where the b_k are phonon amplitudes. The unitary matrix u can be found from symmetry in analogy with the Bloch theorem, without knowledge of particular values of the parameters. Applying periodic boundary conditions with the period L

$$a_{l-L} \equiv a_l \tag{A6}$$

we have the following solution, corresponding to propagating phonons with the wave number k ($k = 1, \ldots, L$)

$$u_{kl} = \frac{1}{\sqrt{L}} \exp\left(i \frac{2\pi kl}{L}\right) \tag{A7}$$

The validity of (A7) can be checked immediately by substitution into (A5a) together with (A1). In the case of real finite MTs we usually have different boundary conditions, for example, zero boundary conditions:

$$a_0 = a_L = 0 \tag{A8}$$

Corresponding normalized eigenvectors describe standing waves:

$$u_{kl} = \sqrt{\frac{2}{L}} \sin\left(\frac{\pi k l}{L}\right) \tag{A9}$$

These amplitudes are represented on Figure 1(i–t) as patterns of the standing wave maxima. Arrows at each site represent the complex amplitudes (A7). We can see the correspondence between *ab initio* calculated phonon modes and experimentally observed patterns of the MAP attachment sites (Figure 1 a–h; Burns, 1978; Kim *et al.*, 1986).

The eigenvalues w_k (normal modes frequencies) can be calculated immediately by substitution of (A1) and (A9) into (A5a). For example, taking the following values of parameters:

$$w_0 = 10^{-5} \text{ eV}, \epsilon_1 = 2 \times 10^{-6} \text{ eV}, \epsilon_2 = 5 \times 10^{-7} \text{ eV}, \epsilon_3 = 10^{-6} \text{ eV} \tag{A10}$$

we have the following frequencies for some of the patterns represented at Figure 1: 1.08 GHz (b), 2.19 GHz (e and o), 2.61 GHz (f and n), 3.23 GHz (m), 2.32 GHz (q), 0.99 GHz (t) (see also Figure 2).

As the period L goes to infinity, we obtain a quasicontinuous spectrum of phonon modes. This spectrum for our particular choice of parameters (A10) with $L = 640$ is represented on Figure 2 as the phonon frequency versus the normalized wave number $æ = k/L$. Each point of this plot stands for a definite phonon mode. For example, the six modes calculated above (Figure 1/t, q, m, e, b and f) are labeled on this plot. However, modes with slightly different æ can have quite different patterns (thus, the pattern e with $æ = 0.3125$ is close to the extremum, Figure 2, but the extremal pattern with $æ = 0.3077$ has the exited line, parallel to the MT axis).

We can see seven phonon bands on the spectrum, the extremums of which correspond to some particular patterns with two or three longitudinal axes. This observation can shed light on the enigmatic rules of the cytoskeleton self-assembling (Bardele, 1977) and will be discussed elsewhere.